Scientia Iranica, Vol. 11, No. 4, pp 351–360

SCIENTIA IRANICA

Dynamic Response of a Moored Semisubmersible in Short-Crested Wave Fields

A. Homayoun Heidari[1], S.M. Borghei[*] and M. Sohrabpour[2]

Wind generated sea states are more accurately modeled by short-crested wave fields. Whether or not these short-crested waves can induce larger response amplitudes in floating offshore structures is of great concern to offshore engineers. In this paper, the hydrodynamics of a moored semisubmersible in short-crested wave fields is investigated. Morison-based motion equations with nonlinear damping terms are used to analyze the dynamic behavior of the structure. A generalized three-parameter short-crested wave field is introduced as the incident wave. The effect of transverse phase lag, wave propagation angle and different ratios of in-line and transverse wave numbers are studied on the force and response amplitudes of the floating structure. Finally, the results are compared to that of the long-crested wave fields and critical cases are specified.

INTRODUCTION

In the investigation of the behavior of floating offshore platforms, one of the main factors is the hydrodynamic force exerted by the incident wave field, which is the major contributive source to the total force experienced by the structure. In most of the research and engineering works in this regard, the wave fields are usually considered long-crested, which means that the waves are infinitely extended in a lateral direction. This is, however, a simplification of the properties and the behavior of the natural wind-generated wave fields.

Generally, a realistic wind-generated sea state is more accurately modeled by three-dimensional wave fields. These wave fields are developed by the interaction of multiple wave components propagating in different directions. Similar to long-crested waves, these wave fields can be considered either irregular or regular. A regular three-dimensional wave field, containing two components propagating at an oblique angle to each other, is called a short-crested sea [1].

The complicated behavior of short-crested waves has received considerable attention from fluid dynamics researchers. Jeffreys [2] presented the properties of nonlinear short-crested wave fields. A second-order solution was obtained by Fuchs [3] and Chappelear [4] calculated a third-order expansion in dimensional form. Hsu et al. [5] presented the formulation of a nonlinear short-crested wave field up to the third-order using a different perturbation parameter and a non-dimensional form. Roberts [1] studied the specifications of highly nonlinear, i.e. very steep, short-crested waves.

The estimation of forces due to short-crested wave fields has been investigated by a few researchers. Zhu [6] presented an analytical study of diffraction of short-crested waves and the resultant wave forces on a vertical circular cylinder. A numerical extension to this study was performed by Zhu and Moule [7], obtaining the results for rectangular and elliptical cross sections as well. Also, the forces on a large surface piercing circular cylinder have been studied by Huntington and Thompson [8]. Recently the forces exerted by second-order short-crested wave fields on a circular cylinder have also been investigated by Zhu and Satravaha [9].

As far as a complex floating offshore structure (such as a semisubmersible) is concerned, a number of researchers have considered the effect of directional seas, with a probabilistic approach, on the response of offshore structures. Different types of structure have been considered, such as a large freely floating box [10] and a TLP [11].

Other authors have also studied the effect of short-crested wave fields on on-shore structures, such as a seawall and a jetty [12,13].

1. *Department of Civil Engineering, North Carolina State University, Campus Box 7908, Raleigh, NC, P.O. Box 27695-7908, USA.*
*. *Corresponding Author, Department of Civil Engineering, Sharif University of Technology, P.O. Box 11365-9313, Tehran, I.R. Iran.*
2. *Department of Mechanical Engineering, Sharif University of Technology, P.O. Box 11365-9313, Tehran, I.R. Iran.*

However, to the authors' knowledge, So far no one has studied the response of a moored compound offshore structure to a deterministic short-crested wave field. In this research work, the behavior of a moored semisubmersible in short-crested wave fields is investigated. A generalized model for a linear deterministic short-crested wave field is introduced, which depends on three parameters. These parameters, for which the parameter study is performed here, are the ratio of wave numbers in in-line and transverse directions, the transverse phase lag and the wave incidence angle, which form the most general definition of regular short-crested wave fields.

The dynamics of the structure is solved in the frequency-domain, considering the nonlinearity of the viscous damping term. The equation of motion is solved in three-dimensions, considering all the six possible degrees of freedom for the structure.

Using the developed computer program based on the strip theory, the effect of the variation of the transverse phase lag on the hydrodynamic forces and the response amplitude of the structure is studied for different wave number ratios. Also, the effect of wave incidence angle on the forces and responses is investigated.

Finally, the results are compared to dynamic responses induced by a long-crested wave field with the same total wave number, to investigate the possibility of larger responses in short-crested wave fields.

WAVE FIELD FORMULATION

A short-crested wave system, as is produced by two progressive waves propagating at an oblique angle to each other, is considered here. Hsu et al. [5] presented the formulation of a short-crested wave field up to third-order by the perturbation method. The field presented by Hsu is defined by the angle between the propagation direction of two regular waves, which form the short-crested wave field by interacting.

A system of Cartesian coordinates with x and y being on a still water level and z pointing upward is considered. Assuming that the resultant wave field is propagating along the x axis, the interaction angle of two progressive waves divides the total wave number between the in-line and transverse direction as:

$$\kappa_x = \kappa \cos\Theta, \quad \text{and} \quad \kappa_y = \kappa \sin\Theta, \tag{1}$$

where κ_x is the in-line wave number (along x axis), κ_y is the transverse wave number (along y axis), κ is the total wave number, which is defined by $\kappa^2 = \kappa_x^2 + \kappa_y^2$ and Θ is the interaction half-angle of two progressive waves, as presented in Figure 1.

The first-order potential function for this short-crested wave field can be written as [6]:

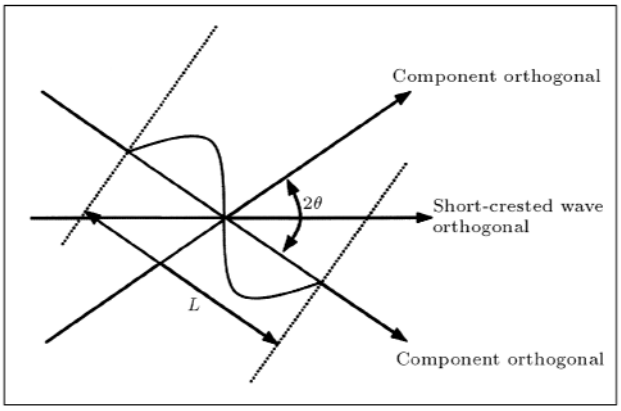

Figure 1. Definition sketch for short-crested wave propagating on x axis. L is the wave length of each component.

$$\phi(x,y,z,t) = \frac{gH}{2\omega}\frac{\cosh(\kappa(z+h))}{\cosh(\kappa h)}\sin(\kappa_x x \quad \omega t)\cos(\kappa_y y), \tag{2}$$

where g is the acceleration of gravity, H is the wave height, h is the water depth, ω is the wave angular frequency and t denotes time. Here, the wave angular frequency is defined by the total wave number using the dispersion relation:

$$\omega^2 = g\kappa \tanh(\kappa h). \tag{3}$$

In addition to the parameters that are needed to describe a regular long-crested wave field, the above-mentioned short-crested wave inherently depends on an additional parameter, which is the interaction angle, Θ.

Moreover, by the definition in Equation 2, the lateral crest is forced to be on the x axis, i.e., $y = 0$. Since the location of this lateral crest can affect the kinematics of the wave field around the structure, the transverse phase lag is introduced, by which, one will be able to set the position of the lateral crest on the y axis.

The generalized short-crested wave field can now be introduced by considering the transverse phase lag and the wave incidence angle as:

$$\phi(x,y,z,t) = \frac{igH}{2\omega}\frac{\cosh(\kappa(z+h))}{\cosh(\kappa h)}\exp\{i(\kappa_{nn}x+\kappa_{nt}y)\}$$

$$\cos(\quad \kappa_{tn}x + \kappa_{tt}y + \theta)e^{\ i\omega t}, \tag{4}$$

where θ is the transverse phase lag, $i = \sqrt{-1}$ and the components of wave numbers are defined as:

$$\begin{cases} \kappa_{nn} = \kappa_n \cos\alpha \\ \kappa_{nt} = \kappa_n \sin\alpha \end{cases} \quad \text{and} \quad \begin{cases} \kappa_{tt} = \kappa_t \cos\alpha \\ \kappa_{tn} = \kappa_t \sin\alpha \end{cases}, \tag{5}$$

where α is the wave propagation angle relative to x axis, κ_n is the in-line wave number (along the

propagation direction) and κ_t is the transverse wave number. Note that the $n \quad t$ axis has an angle of α with the $x \quad y$ axis defined above.

The above short-crested wave field can now be defined by three independent parameters, namely the ratio of wave numbers of in-line and transverse directions, the wave propagation angle and the transverse phase lag. The wave number ratio, which is defined as:

$$\mu = \frac{\kappa_t}{\kappa_n}, \tag{6}$$

can vary from zero, which is the case of a long-crested wave field with κ_n being the total wave number and $\kappa_t = 0$ up to very large numbers, which present very short-crested wave fields.

The kinematics of the short-crested wave field can now be defined in a matrix form as:

$$\begin{Bmatrix} u \\ v \\ w \end{Bmatrix} = \frac{gH}{2\omega} \frac{\cosh(\kappa(z+h))}{\cosh(\kappa h)} e^{i(\kappa_{nn}x + \kappa_{nt}y)} \begin{bmatrix} \kappa_{nn} & i\kappa_{tn} \\ \kappa_{nt} & i\kappa_{tt} \\ i\kappa \tanh(\kappa(z+h)) & 0 \end{bmatrix} \begin{Bmatrix} \cos\chi \\ \sin\chi \end{Bmatrix} e^{\ i\omega t}, \tag{7}$$

and:

$$\begin{Bmatrix} \dot{u} \\ \dot{v} \\ \dot{w} \end{Bmatrix} = \frac{gH}{2} \frac{\cosh(\kappa(z+h))}{\cosh(\kappa h)} e^{i(\kappa_{nn}x + \kappa_{nt}y)} \begin{bmatrix} i\kappa_{nn} & \kappa_{tn} \\ i\kappa_{nt} & \kappa_{tt} \\ \kappa \tanh(\kappa(z+h)) & 0 \end{bmatrix} \begin{Bmatrix} \cos\chi \\ \sin\chi \end{Bmatrix} e^{\ i\omega t}, \tag{8}$$

where u, v, w are the particle velocities in x, y and z directions, respectively, $\dot{u}, \dot{v}$ and $\dot{w}$ are the particle accelerations in x, y and z directions, respectively and χ is the transverse phase expressed as:

$$\chi = \quad \kappa_{tn}x + \kappa_{tt}y + \theta. \tag{9}$$

Based on the above model, the first-order dynamic wave pressure due to the short-crested wave system can be defined by the following equation:

$$p_d(x,y,z,t) = \frac{\rho g H}{2} \frac{\cosh(\kappa(z+h))}{\cosh(\kappa h)} \exp\{i(\kappa_{nn}x + \kappa_{nt}y)\} \cos(\chi) e^{\ i\omega t}, \tag{10}$$

where ρ is the density of the sea water.

DYNAMIC ANALYSIS

The dynamic response equation for the rigid body motion of the semisubmersible in six degrees of freedom is written based on the Morison loading model. The elongated members of the structure are discretized into small elements to account for the variation of water particle velocities and accelerations.

The general response equation of the moored semisubmersible may be expressed in the following matrix form:

$$\mathbf{M}\ddot{\mathbf{X}} = \sum_j \mathbf{M}_a^j(\ddot{\xi} \quad \ddot{\mathbf{X}}) + \sum_j \mathbf{F}_{FK}^j + \sum_j \mathbf{B}^j|\dot{\xi} \quad \dot{\mathbf{X}}|(\dot{\xi} \quad \dot{\mathbf{X}}) \quad (\mathbf{K}_h + \mathbf{K}_m(\mathbf{X}))\mathbf{X}, \tag{11}$$

where $\mathbf{M}$ is the physical mass matrix of the structure (6×6), j is the element index, $\mathbf{M}_a^j$ and $\mathbf{B}^j$ are the added mass and nonlinear damping matrices for the jth element, respectively (6×6), $\mathbf{X}, \dot{\mathbf{X}}$ and $\ddot{\mathbf{X}}$ are the vectors of displacement, velocity and acceleration of the center of gravity of the structure, respectively (6×1), $\mathbf{K}_h$ is the hydrostatic stiffness matrix (6×6), $\mathbf{K}_m(\mathbf{X})$ is the nonlinear stiffness matrix of the mooring system calculated by the instantaneous structural motion (6×6), $\dot{\xi}$ and $\ddot{\xi}$ are the particle velocity and acceleration vectors, respectively (6×1) and $\mathbf{F}_{FK}^j$ is the Froude-Krylov force vector on the jth element (6×1). It should be noted that since the flow field is assumed to be irrotational, the particle velocity and acceleration vectors have only three non-zero elements corresponding to the translational degrees, which are defined in Equations 7 and 8.

In order to decouple the motion of the structure and the velocity vector in a nonlinear damping term, Matsushima et al. [14] presented an approximated formulation, which lead to the following restructured motion equation:

$$(\mathbf{M} + \mathbf{M}_a^t)\ddot{\mathbf{X}} + \mathbf{B}^t|\dot{\mathbf{X}}|\dot{\mathbf{X}} + (\mathbf{K}_h + \mathbf{K}_m(\mathbf{X}))\,\mathbf{X} = \mathbf{F}(t), \tag{12}$$

in which $\mathbf{M}_a^t$ is the total added mass matrix of the structure, $\mathbf{B}^t$ is the total nonlinear damping matrix of the structure and $\mathbf{F}(t)$ is the time-dependent force vector, expressed as:

$$\mathbf{F}(t) = \sum_j \mathbf{M}_a^j \ddot{\xi} + \sum_j \mathbf{F}_{FK}^j + \sum_j \mathbf{B}^j|\dot{\xi}|\dot{\xi}. \tag{13}$$

The above equation can be solved using time-domain techniques but in the frequency-domain, which is the interest of the present research, the nonlinear damping terms should be linearized. The work-equivalent method can be used for the linearization of the damping terms [15], which results in the following motion equation:

$$(\mathbf{M} + \mathbf{M}_a^t)\ddot{\mathbf{X}} + \mathbf{B}_e^t|\dot{\mathbf{X}}_0|\dot{\mathbf{X}} + (\mathbf{K}_h + \mathbf{K}_m(\mathbf{X}))\mathbf{X} = \mathbf{F}(t), \tag{14}$$

where $\mathbf{B}_e^t$ is the linearized damping matrix and is defined as $\mathbf{B}_e^t = 8\mathbf{B}^t/3\pi$ and $\dot{\mathbf{X}}_0$ and $\dot{\xi}_0$ are the amplitude vectors of velocity of the structure and water particles, respectively. Furthermore, the force vector $\mathbf{F}(t)$ can be rewritten as:

$$\mathbf{F}(t) = \sum_j \mathbf{M}_a^j \ddot{\xi} + \sum_j \mathbf{F}_{FK}^j + \sum_j \mathbf{B}_e^j |\dot{\xi}_0| \dot{\xi}, \tag{15}$$

in terms of linearized damping.

The motion Equation 14 may now be transformed into the frequency-domain by considering the oscillatory nature of both the motion of the structure and the loading term as:

$$\begin{cases} \mathbf{X} = \mathbf{X}_0(\omega) e^{\ i\omega t} \\ \mathbf{F} = \mathbf{F}_0(\omega) e^{\ i\omega t} \end{cases}, \tag{16}$$

where $\mathbf{X}_0(\omega)$ and $\mathbf{F}_0(\omega)$ are the amplitudes of motion and force, respectively. The equation can now be solved by an iterative technique, to account for the nonlinearity in damping terms. Based on Equation 16, the motion equation will be reduced to the following form:

$$\Omega(\omega).\mathbf{X}_0(\omega) = \mathbf{F}_0(\omega), \tag{17}$$

where $\Omega(\omega)$ is the frequency-dependent coefficient matrix and $\mathbf{F}_0(\omega)$ is the vector of force amplitude, which are defined as:

$$\Omega(\omega) = \left[\omega^2(\mathbf{M}+\mathbf{M}_a^t) + (\mathbf{K}_h + \mathbf{K}_m(\mathbf{X})) \quad i\omega \mathbf{B}_e^t |\dot{\mathbf{X}}_0^p| \right]_{6\times 6}, \tag{18}$$

$$\mathbf{F}_0(\omega) = \left[\sum_j \mathbf{M}_a^j \ddot{\xi}_0 + \sum_j (\mathbf{F}_{FK}^j)_0 + \sum_j \mathbf{B}_e^j |\dot{\xi}_0| \dot{\xi}_0 \right]_{6\times 1}. \tag{19}$$

respectively. In the above equations, $\ddot{\xi}_0$ is the amplitude vector of water particle acceleration, $(F_{FK}^j)_0$ is the amplitude vector of the Froude-Krylov hydrodynamics force on the jth element and $\mathbf{X}_0^p$ denotes the velocity amplitude of the structural motion calculated at the previous iteration step.

Here, the mooring system stiffness matrix is calculated based on the actual excursion of the structure from the equilibrium position at each iteration step. Therefore, the nonlinear behavior of the mooring lines during large motions would be taken into account.

RESULTS

A computer program for frequency-domain response analysis of moored offshore structures, based on the above-described method of dynamic analysis and the generalized short-crested wave field model, is developed. The geometry of the structure is imported into the program, based on super elements such as columns or pontoons. The discretization of the elongated members is performed automatically by the program, given the degree of accuracy. For the mooring system, a general spread mooring is considered where the geometry of the mooring lines and other physical specifications are among the inputs of the program.

The hydrodynamic forces and moments on the structure and the response amplitude of the semisubmersible are calculated within the specified range of frequencies using a unit wave height. Figure 2 shows

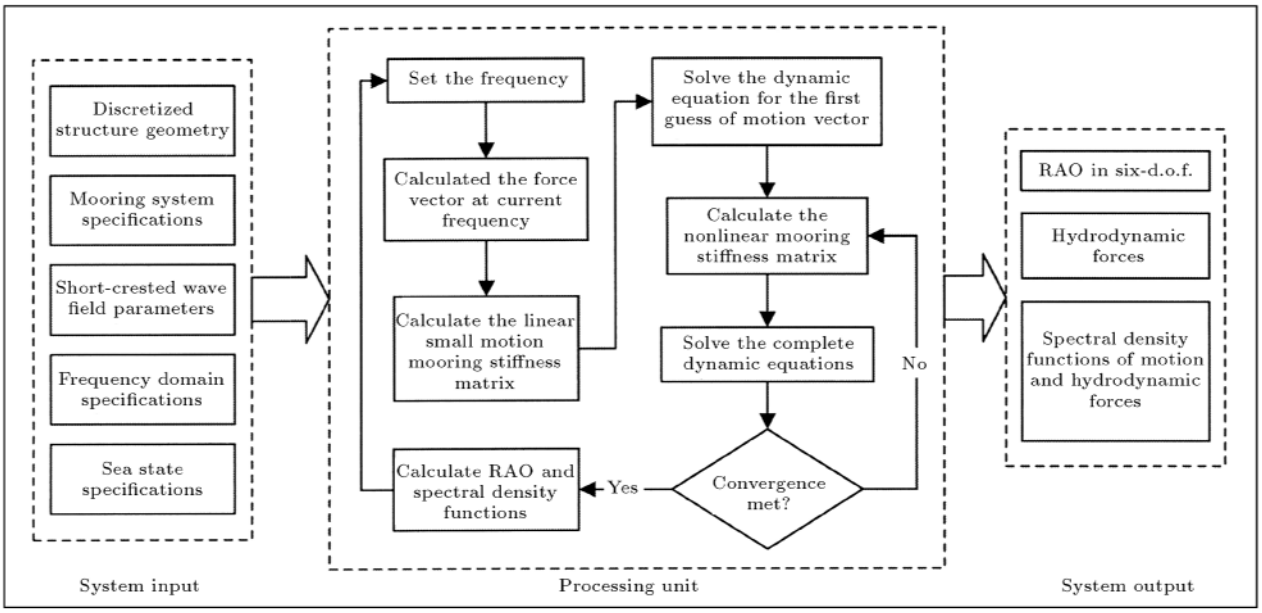

Figure 2. The data flow and solution process diagram of the computer code.

the data flow and an overview of the solution procedure in the code.

The results are presented for a semisubmersible moored to the sea bottom by a symmetrical spread mooring system containing eight mooring lines. The geometrical specifications of the structure and the mooring system layout of the semisubmersible are illustrated in Figure 3.

In the following study, three cases for the wave number ratio are considered. The first one is a unit wave number ratio ($\mu = 1.0$) that generates a similar pattern of wave crests in both in-line and transverse directions. The second case is $\mu = 0.6$, which is the case for $\kappa_t < \kappa_n$ and corresponds to a larger wavelength along the transverse direction. Finally $\mu = 1.5$ is considered, which is approximately the opposite situation of the previous case and simulates a case of $\kappa_t > \kappa_n$.

Since the energy of a short-crested wave field is distributed in two horizontal directions, namely in-line and transverse, a proper way to investigate and compare the horizontal forces and response of the structure to the one of the long-crested wave fields, is to use the resultant horizontal motion and forces caused by both surge and sway degrees of freedom, which are calculated as:

$$x_r = \sqrt{\mathbf{X}_1^2 + \mathbf{X}_2^2} \quad \text{and} \quad f_r = \sqrt{\mathbf{F}_1^2 + \mathbf{F}_2^2}, \tag{20}$$

where the subscripts 1 and 2 denote the first and second elements of the displacement and force vectors corresponding to the two horizontal degrees of freedom.

Therefore in the following graphs, the horizontal resultant degree is used as a substitute for two translational horizontal degrees, namely surge and sway, both for forces and for responses. However, to illustrate the activation of transverse motion, the response of the sway mode is also included on the graphs.

Effect of Transverse Phase Lag

Here, the effect of transverse phase lag in each of the above mentioned cases for μ is investigated. Three values for transverse phase lag is considered, namely $\theta = 0°$, $45°$ and $90°$.

Figures 4 and 5 show the hydrodynamic forces and moments in different directions and the response amplitude operators for different modes of motion for the case of $\mu = 0.6$. The graphs show that the forces and responses in the horizontal resultant component are both greater for $\theta = 0°$ and the peak frequencies only slightly differ for various phase lags. This is also true for heave force and response, except for $\theta = 90°$

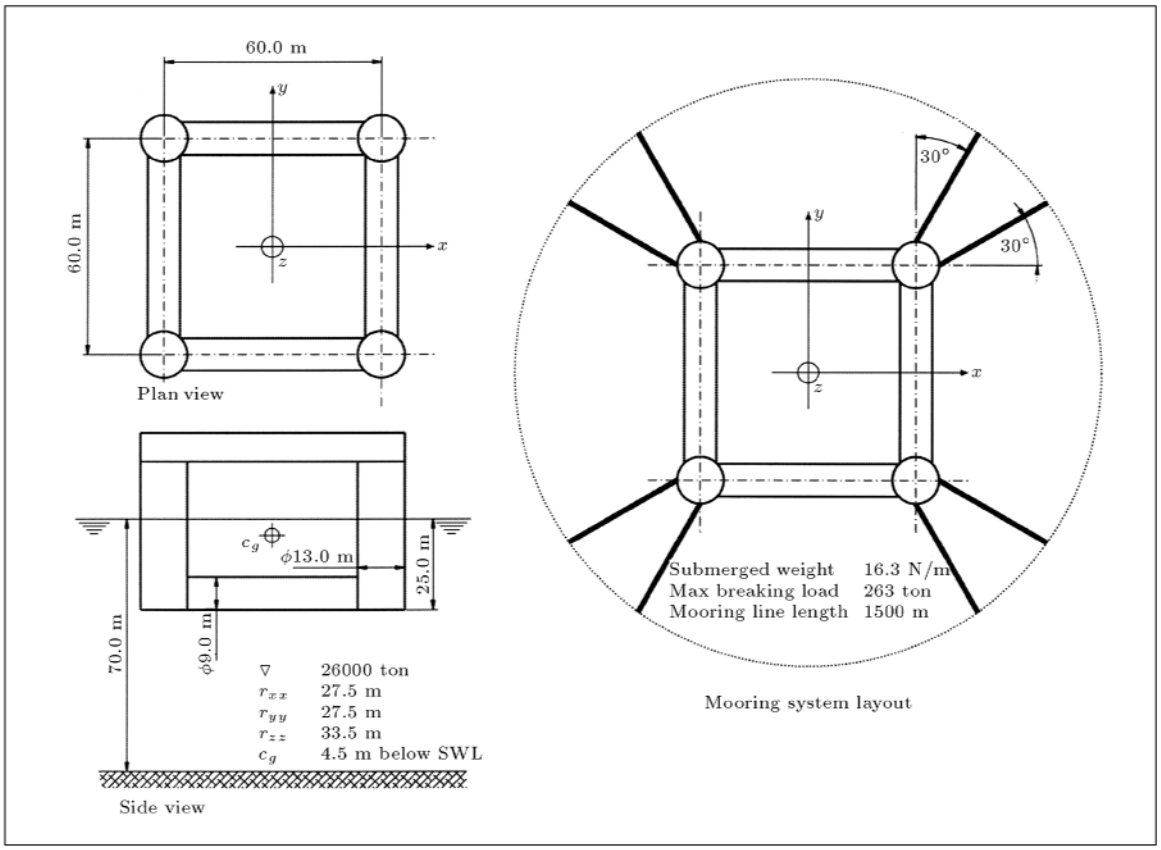

Figure 3. The geometrical specifications and mooring system layout of the semisubmersible.

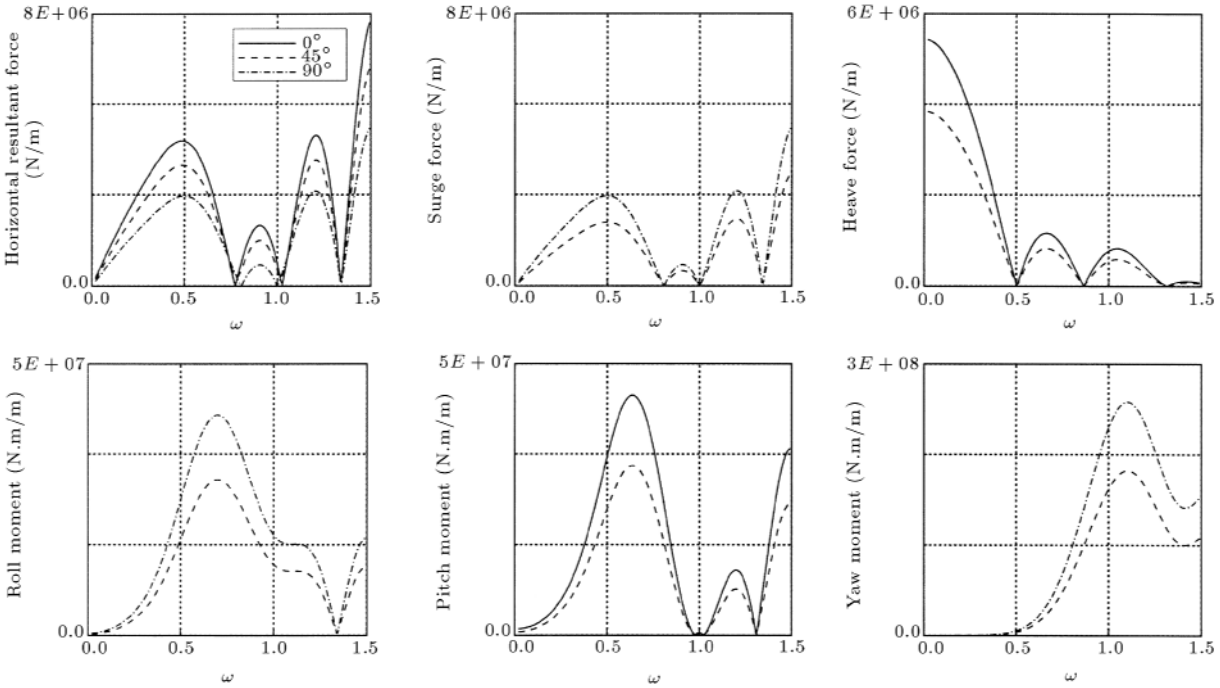

Figure 4. The hydrodynamic forces and moments for different values of transverse phase lag, $\mu = 0.6$ and $\alpha = 0°$.

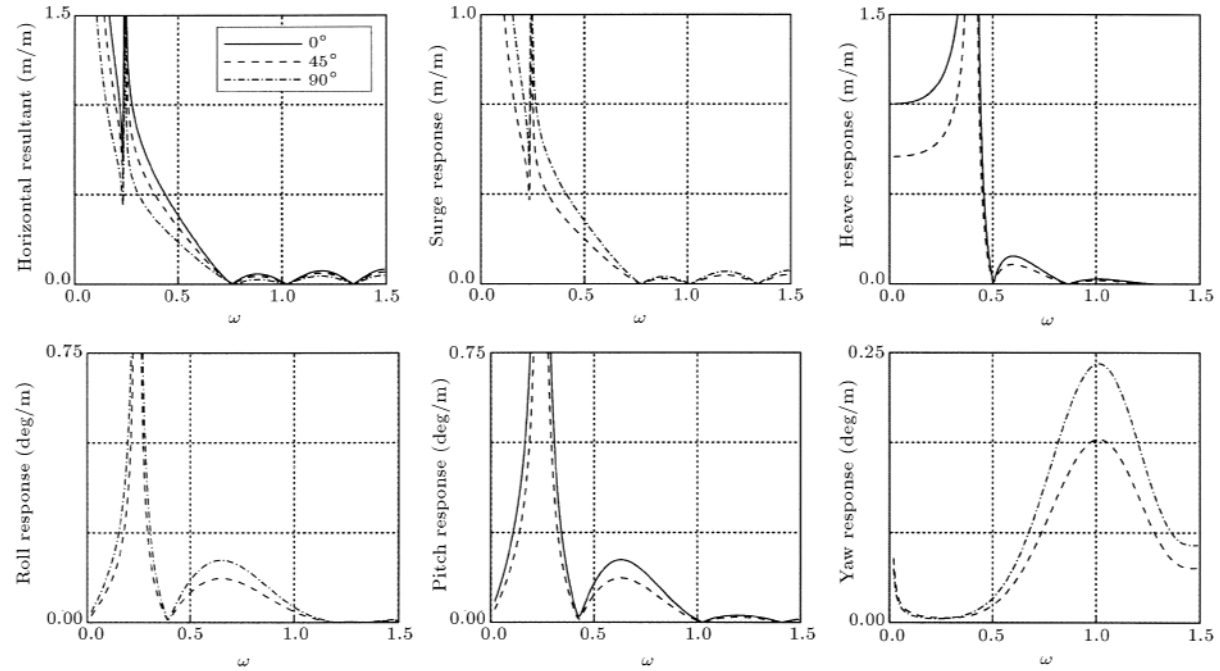

Figure 5. The response amplitude operators for different values of transverse phase lag, $\mu = 0.6$ and $\alpha = 0°$.

where heave motion no longer exists. In fact, in the case of $\theta = 90°$, the vertical forces in positive and negative sides of the x axis cancel each other but, on the other hand, the roll moment reaches its maximum value over the whole range of frequency. The roll is not activated at $\theta = 0°$. The pitch moment and response follow the same pattern as the heave mode. The behavior of the yaw degree of freedom is the same as the roll as it reaches its maximum at $\theta = 90°$ and it is dormant at $\theta = 0°$.

Figure 6 shows the response amplitude of the structure in the case of unit wave number ratio, $\mu = 1.0$. As can be immediately concluded from the graphs, the horizontal motion is not sensitive to the transverse

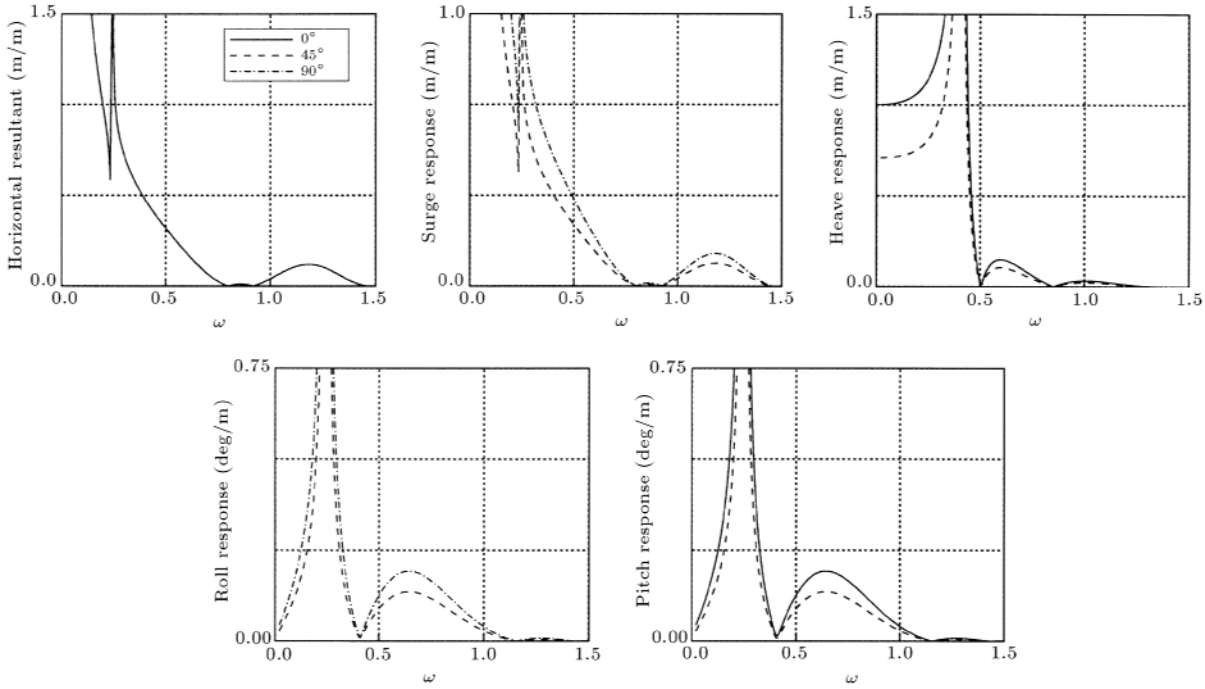

Figure 6. The response amplitude operators for different values of transverse phase lag, $\mu = 0.1$ and $\alpha = 0°$. The yaw response is absent due to symmetry of wave pattern around the structure.

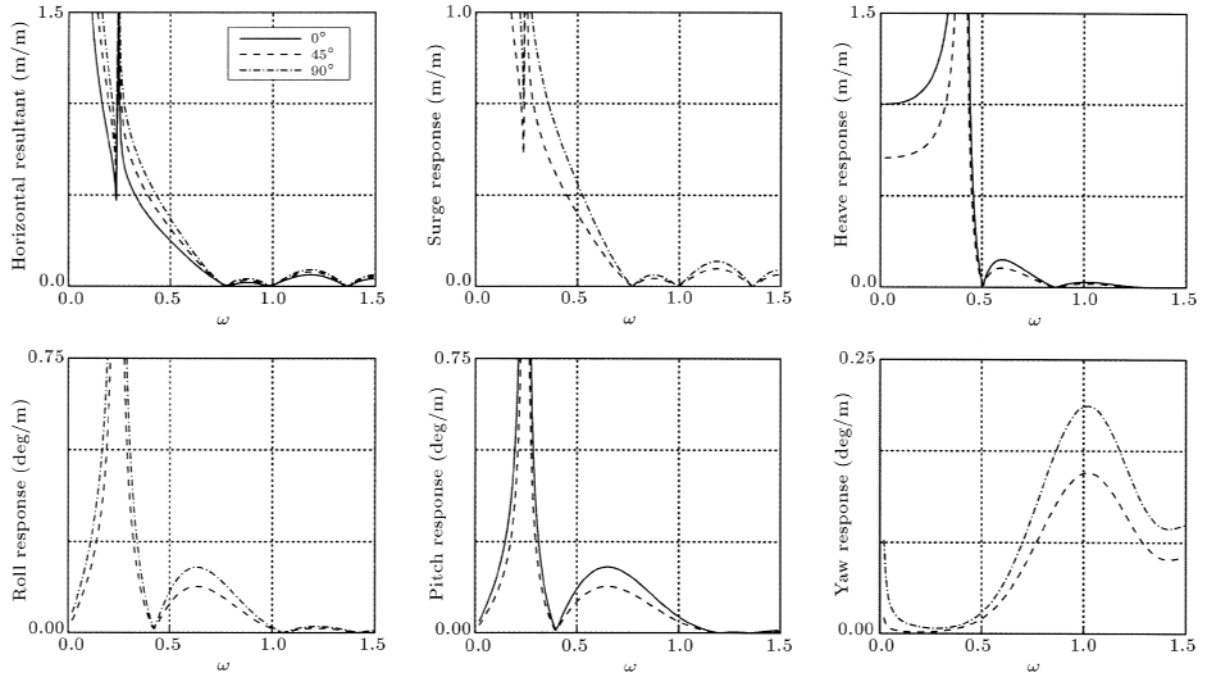

Figure 7. The response amplitude operators for different values of transverse phase lag, $\mu = 1.5$ and $\alpha = 0°$.

phase lag, which is expected. The heave, roll and pitch motions show the same pattern as the previous case of $\mu < 1$. The yaw motion is at rest in this case, even for $\theta > 0$, due to the symmetry of the wave pattern.

The last case, $\mu = 1.5$, is illustrated in Figure 7. The horizontal resultant shows an exactly opposite behavior to that of $\mu < 1$, having its maximum response in $\theta = 90°$. Other degrees of freedom show the same trend of change with θ, as in other values of the wave number ratio.

Effect of Wave Incidence Angle

Using the obtained trend about the sensitivity of forces and motions to the transverse phase lag value, the study of the effect of the wave incidence angle is limited to those cases of θ in which the corresponding response amplitude operator is maximized. The effect of the wave incidence angle is investigated based on three values, namely: $\alpha = 0°$, $30°$ and $60°$. For each value of the wave number ratio, the results of different wave incidence angles are presented. For the sake of brevity, only the motion response amplitudes are presented.

Figure 8 shows the effect of wave incidence angle in case of $\mu < 1$. The horizontal resultant motion response for both $30°$ and $60°$ are the same and are mostly larger than that of head sea, except in a small range of frequencies around $\omega \cong 1.4$ rad/sec. The roll and pitch degrees have greater response amplitude for head sea in most of the frequency range, compared to those of an oblique incidence of waves. The transverse phase lag is declared at each graph.

The case of $\mu = 1.0$ is illustrated in Figure 9. It is obvious that due to the symmetry of the wave pattern in this case, both oblique seas have the same response curve for horizontal resultant motion. Both angles of incidence exert, approximately, the same peak response compared to that of head sea, except that the peak frequency is shifted to a lower value. The roll and pitch motions have their maximum response curve in head sea, just like the case of $\mu < 1.0$. The yaw moment, which was at rest in $\mu = 1.0$ for head sea, shows a notable response for oblique seas.

The case of $\mu = 1.5$ is shown in Figure 10, where horizontal motion has its maximum response peak in the case of oblique waves and a lower peak frequency than that of head sea. The roll and pitch again show the same behavior by having their maximum response

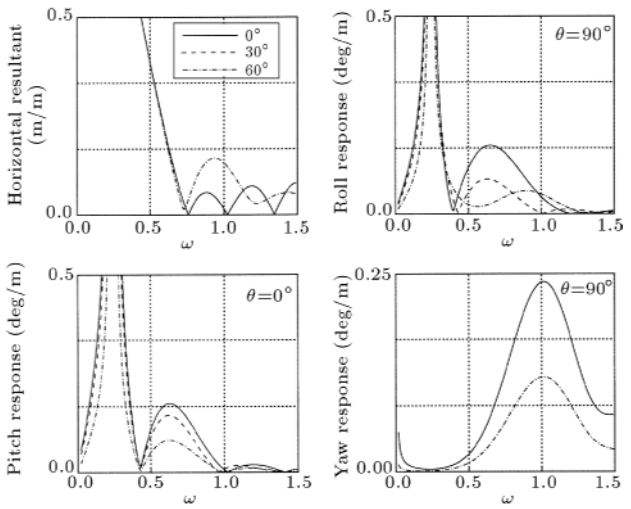

Figure 8. The response amplitude operators for different values of wave incidence angle, $\mu = 0.6$.

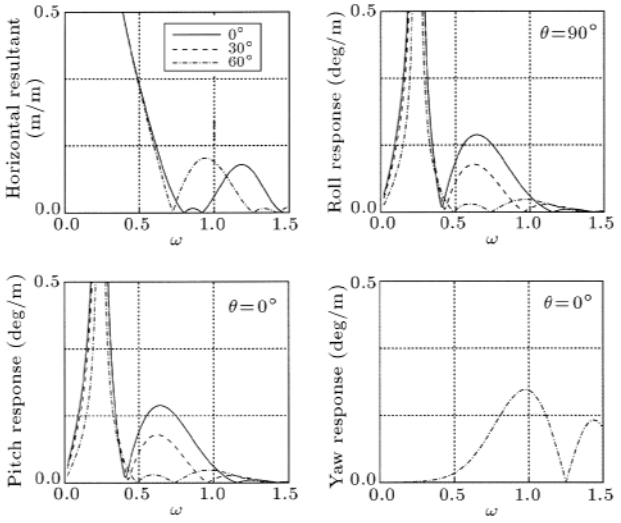

Figure 9. The response amplitude operators for different values of wave incidence angle, $\mu = 1.0$.

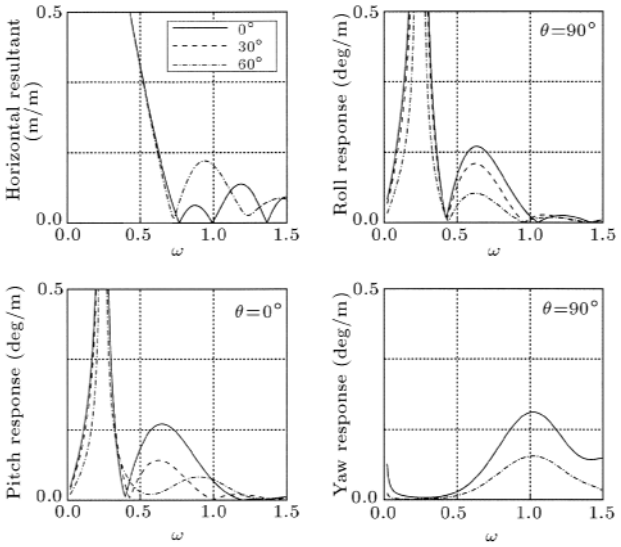

Figure 10. The response amplitude operators for different values of wave incidence angle, $\mu = 1.5$.

in head sea over the whole range of frequency. Finally, the yaw moment has its maximum response curve in head sea and an equal behavior for both oblique angles of wave incidence.

In none of the above cases, a considerable sensitivity of heave response to wave incidence angle has been observed, as expected.

Comparison with Long-Crested Wave Field

According to the previously described results on the effect of transverse phase lag, comparisons will be made between the response of the semisubmersible in long- and short-crested wave fields for both cases of $\theta = 0°$ and $90°$.

The first case, illustrated in Figure 11, shows the

response curves for different values of the wave number ratio, in case of no transverse phase lag, i.e., $\theta = 0°$. Only four selected graphs, which show considerable deviation between long- and short-crested results, are shown in this figure.

It can be concluded from the graphs that the response to the short-crested wave field is considerably higher than that of the long-crested, in case of a 30° incidence angle in the mid-frequencies range. There is also a small range of frequency, in which the response is higher for a short-crested wave in a head sea. However, in other regions, the horizontal resultant motion is mostly higher for a long-crested incident wave.

The pitch response in a short-crested sea is notably higher for the mid-frequency range in the head sea, but still lower in low frequencies.

Finally, the yaw moment for a short-crested field in $\theta = 0°$ and $\alpha = 30°$, is nearly equal to that of the long-crested waves, but, in the high frequencies, i.e. around $\omega = 1.5$ rad/sec, it is almost doubled.

Figure 12 shows another set of graphs which illustrate the case of $\theta = 90°$. The same situation governs the horizontal resultant motion degree, where the response to the short-crested wave field is higher for an oblique sea around the mid-frequency range and lower for most of the other regions. The roll motion is illustrated for head sea. This mode, which is dormant in cases of long-crested wave fields, is activated in short-crested wave fields. The same goes for the yaw motion degree, where it is activated and notably high for the short-crested field and dormant for long-crested waves.

CONCLUSION

In the present paper, the response of a moored semisubmersible to a short-crested wave field is analyzed. The effect of the transverse phase lag and the wave incidence angle of a short-crested sea on the response of the vessel in different wave number ratios are studied. Finally the critical cases are designated and compared with the response of the vessel in a long-crested wave field.

In a symmetric loading, the values of the transverse phase lag affect the activation and response amplitude of some degrees of freedom that are at rest in a long-crested wave field loading.

The response of the vessel in a short-crested wave field is highly affected by the value of angle of incidence. An oblique sea induces a higher response in the horizontal resultant motion and a lower response in other modes of motion.

The horizontal resultant motion is more excited in an oblique short-crested sea, compared to long-crested waves with the same incidence angle, while, in head sea, it is higher for long-crested waves over most of the frequency range. The pitch motion is also higher in short-crested waves within the mid-frequency range for head seas. Also, the roll and yaw motion, which are at rest for head sea in long-crested wave fields, becomes activated and considerably high (in case of roll) for a short-crested sea. Furthermore, in short-crested seas, the heave motion of the vessel is always equal or lower than that of the long-crested wave field. The transverse phase lag has a reducing effect on heave motion, by shifting a portion of the energy of this mode to roll and pitch degrees of freedom.

Finally, it can be concluded that short-crested wave fields can induce higher dynamic response amplitudes in moored vessels in certain degrees of freedom and in certain ranges of frequency. Therefore, its effect on certain items of design criteria, such as limitations on horizontal acceleration, rotation amplitude and mooring line forces, should be studied more explicitly.

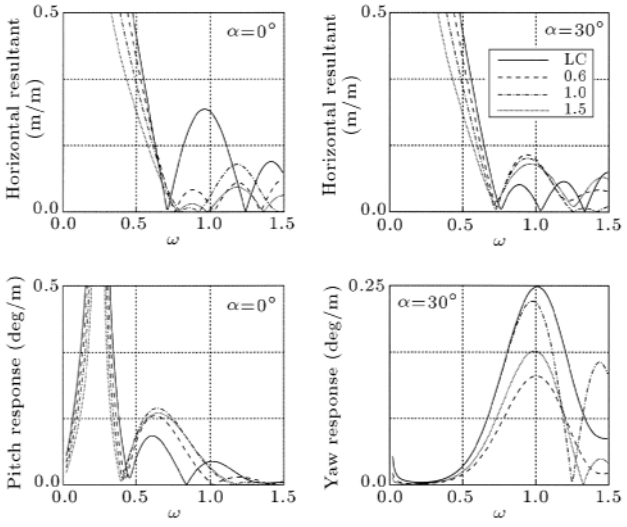

Figure 11. Response of the structure in long- and short-crested wave fields, $\theta = 0°$.

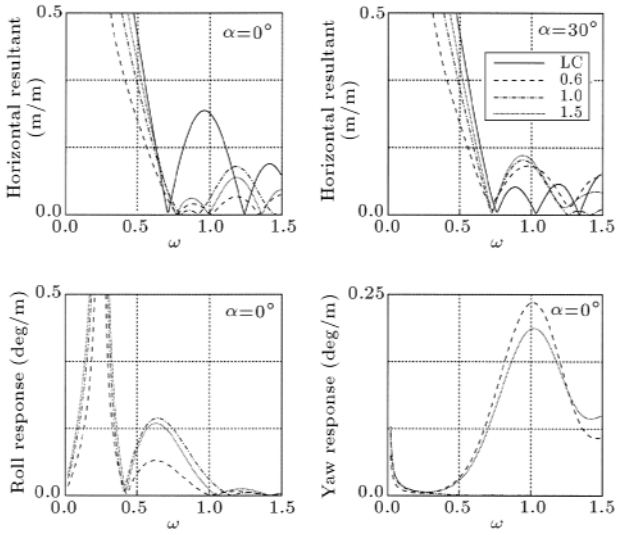

Figure 12. Response of the structure in long- and short-crested wave fields, $\theta = 90°$.

ACKNOWLEDGMENTS

The authors would like to express their sincere thanks to Professor A. Incecik from the Department of Marine Technology of the University of Newcastle-Upon-Tyne, UK, for many helpful discussions and suggestions. They, also, would like to thank Professor A.N. Williams from the Department of Civil Engineering at the University of Houston, Texas, for his careful review and constructive observations for the improvement of this paper during A.H. Heidari's visit to the University of Houston.

REFERENCES

1. Roberts, A.J. "Highly non-linear short-crested water-waves", *J. Fluid Mech.*, **135**, pp 301-321 (1983).
2. Jeffreys, H. "On water waves near the coast", *Phil. Mag.*, Ser., **6**(17), pp 44-48 (1924).
3. Fuchs, R.A. "On the theory of short-crested oscillatory waves: Gravity waves", *National Bureau of Standard*, Circular No. 8, pp 187-200 (1952).
4. Chappelear, J.E. "On the description of short-crested waves", *Beach Erosion Board, U.S. Army Corps of Engineers*, Memo No. 125, pp (1961).
5. Hsu, J.R.C. et al. "3rd-order approximation to short-crested waves", *J. Fluid Mech.*, **90**, pp 179-196 (1979).
6. Zhu, S.P. "Diffraction of short-crested waves around a circular-cylinder", *Ocean Eng.*, **20**(4), pp 389-407 (1993).
7. Zhu, S.P. and Moule, G. "Numerical-calculation of forces induced by short-crested waves on a vertical cylinder of arbitrary cross-section", *Ocean Eng.*, **21**(7), pp 645-662 (1994).
8. Huntington, S.W. and Thompson, D.M. "Forces on large cylinder on multidirectional random waves", *Proceedings of Offshore Technology Conference*, Houston, TX, **II**, pp 169-183 (1976).
9. Zhu, S.P. and Satravaha, P.C. "2nd-order wave diffraction forces on a vertical circular-cylinder due to short-crested waves", *Ocean Eng.*, **22**(2), pp 135-189 (1995).
10. Isaacson, M.D. and Sinha, S. "Directional wave effects on large offshore structures", *J. Waterway Port Coast. Ocean Eng.-ASCE*, **112**(4), pp 482-497 (1986).
11. Teiegn, P.S. "The response of TLP in short-crested waves", *Proceedings of Offshore Technology Conference*, Houston, TX, **III**, pp 525-532 (1983).
12. Battjes, A.J. "Effect of short-crestedness on wave loads on long structures", *Appl. Ocean Res.*, **4**, pp 165-172 (1982).
13. Fenton, J.D. "Short-crested waves and the wave forces on a wall", *J. Waterway Port Coast. Ocean Eng.-ASCE*, **111**, pp 693-718 (1985).
14. Matsushima et al. "Seakeeping of a semisubmerged catamaran (SSC) vessel", *Journal of the Society of Naval Architects of West-Japan* (March 1982).
15. Patel, M.H. and Witz, J.A., *Compliant Offshore Structures*, Butterworth-Heinmann Ltd., Oxford, Uk (1991).